Roinn Cumarsáide, Gníomhaithe ar son na hAeráide & Comhshaoil
Department of Communications, Climate Action & Environment

Geological Survey
Suirbhéireacht Gheolaíochta
Ireland | Éireann

Research Programme
- Short Call 2020, Final Report -

Lead Applicant Name	Dr Duygu Kiyan
Host Organisation Name	Dublin Institute for Advanced Studies
Project Title	RAFTA: **R**esolution **A**nalyses for **F**requency- and **T**ime-Domain **A**irborne Electromagnetic Data of the Irish Tellus Programme
Contract Number	2020-sc-049

This report covers the period 1st December 2020 to project end date 31st August 2022)

2. (a) Project information:

Final project report

Executive summary:

The aim of the project RAFTA is to further develop the existing *aempy* toolbox for a better understanding of the uncertainties in AEM data inversion. We have transferred practically all of the original *aempy* toolbox to Python 3.8+, taking advantage of the much-improved external toolboxes of this ecosystem (e.g., numpy, scipy, matplotlib, gdal). The toolbox can now be used with Anaconda-like setups on Windows systems. In addition, we have implemented some new methods, which are particularly adapted for the quantification of uncertainties and are based on the traditional and ensemble type inversions. For the first time, we were successful in using our tools on the GENESIS time-domain data. Our analysis demonstrated that in general only the vertical component of the field data can be inverted, because of the frequent occurrence of negative data in the in-line component. We performed a comparison of the frequency and time-domain methods on synthetic data, and on field data from two survey areas in (Bundoran, Co. Donegal and Clara, Co. Offaly), where ERT data existed or were measured under the framework of the RAFTA project. Although frequency- and time-domain field data inversions have not produced consistent models, comparison of ERT and time-domain AEM-derived models shows a good agreement at greater depths. The resolution of the ERT data was noticeably higher in the shallower subsurface, particularly where a thin conductive layer (30Ωm) occurred within the first 10m depth. The Tellus FDEM data successfully resolved the conductivity of the top layer only, which is in good agreement with the ERT model.

(i) Results, scientific/engineering targets reached beyond the state of the art and conclusions

The Tellus airborne geophysical programme in Ireland started with the first airborne geophysical survey of Northern Ireland, which was flown in 2005 and 2006. It soon was complemented with the Tellus Border project covering five of the six northern most counties of the Republic of Ireland in 2011 to 2012. In the following years, five more surveys were completed, so that, to date, more than 50% of the island of Ireland has been covered. AEM data have been acquired using time-domain (TD) and frequency-domain (FD) systems (Figure 1). Representing a wealth of information on the electrical conductivity structure of Ireland's near surface motivated us to develop tools to improve their interpretation under the framework of 2015 GSI Short Call (2015-sc-04). We have developed a fully open-source toolbox, *aempy*, coded in Python language for the one-dimensional inversion of AEM data along the flight lines (Kiyan et al., 2022).

GSI has produced and made available to the public EM resistivity inversion models computed using the *aempy* code and are available for download from GSI's website (https://www.gsi.ie/en-ie/data-and-maps/Pages/Geophysics.aspx). The *aempy* code is also freely available to all Tellus data users wishing to produce their own EM inversion models from the EM source data. Currently, however, the resolution capabilities of the two Tellus EM systems used and the resolution of the resistivity models themselves is poorly known, which restricts the confidence with which the models might be interpreted and limits the geological value that might be derived from them. The overarching objective of the RAFTA project is to develop a workflow for uncertainty and resolution analyses of FD and TD AEM data and models.

In the following subsections, inversion results from both FD and TD AEM systems and the influence of flight altitude parameters and data error assumptions on the resulting inverted subsurface models are discussed using synthetic and co-located Tellus AEM datasets. Additionally, with the aim of investigating how the resistivity structure of the subsurface along the Tellus AEM profiles compares with ground data, an Electrical Resistivity Tomography (ERT) survey was carried out in September 2022 along a 470 m portion of a co-located Tellus AEM profile.

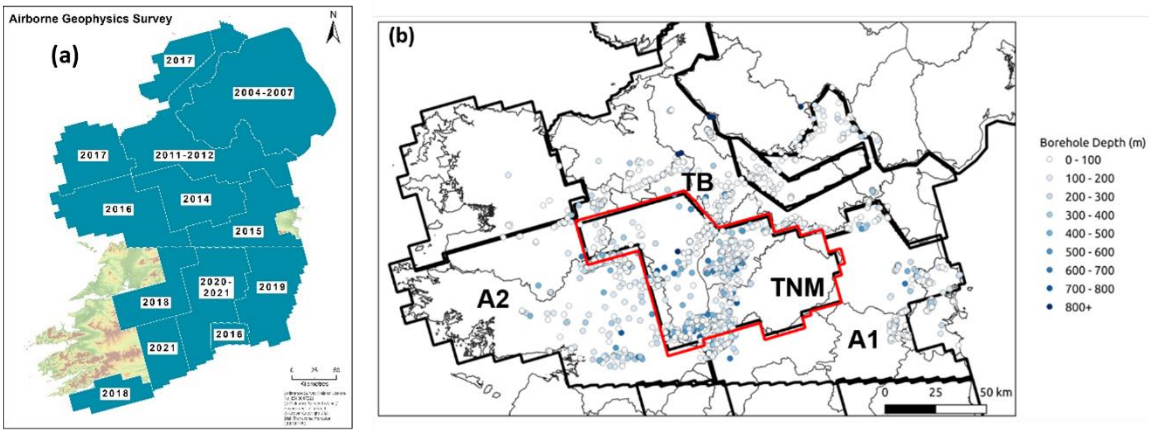

Figure 1: (a) Map showing the outlines of the Tellus survey blocks to date against the backdrop of Irish counties. 2014 polygon shows Tellus North Midlands (TNM) block. (b) Tellus survey blocks together with boreholes from the GSI "verified" borehole database. Time-domain airborne EM data are available within the TNM survey block and frequency-domain AEM data are available within the TB (Tellus Border), A1 and A2 survey blocks.

Synthetic AEM Data

This section discusses the forward modelling responses of both FD and TD synthetic data simulated based on two different three-layer earth models (Bayat, 2023, M.Sc. Thesis). Idealised 1-D earth models, used in this study, assume that all isotropic horizontal layers are electrically homogeneous. The simulation results of the models are inverted and, then the effect of flight altitude and inversion parameters (i.e., data error assumption) on the inversion results are discussed.

Synthetic FD and TD data for two different three-layer subsurface models are shown in Figure 2A and B. Figure 3 summarises the Tikhonov-type inversion results of synthetic FD data for the simple three-layer resistivity model illustrated in Figure 2A. The simulated airborne system is the one used for the Tellus surveys: two pairs of co-planar coils operating at four frequencies with TX – RX separation of ≈ 21.4m. In-phase and quadrature components were randomly perturbed with the noise of 30ppm.

The data were inverted using 1-D smooth, multi-layer Tikhonov-type inversion (Kiyan et al., 2022). The inversion results for the altitudes of 60m, 90m, and 150m are presented on Figure 3. Inverted models indicate that the resistivity values of the first and second layers are estimated with a relatively acceptable approximation for the low-flight altitudes (i.e., 60m and 90m). The resistivity of the bottom layer has not been precisely recovered due to the presence of a highly conductive middle layer which has a strong impact on the resolution of the bottom layer. For the higher altitude, 150m, there is a noticeable deviation from the true model for each of the three layers.

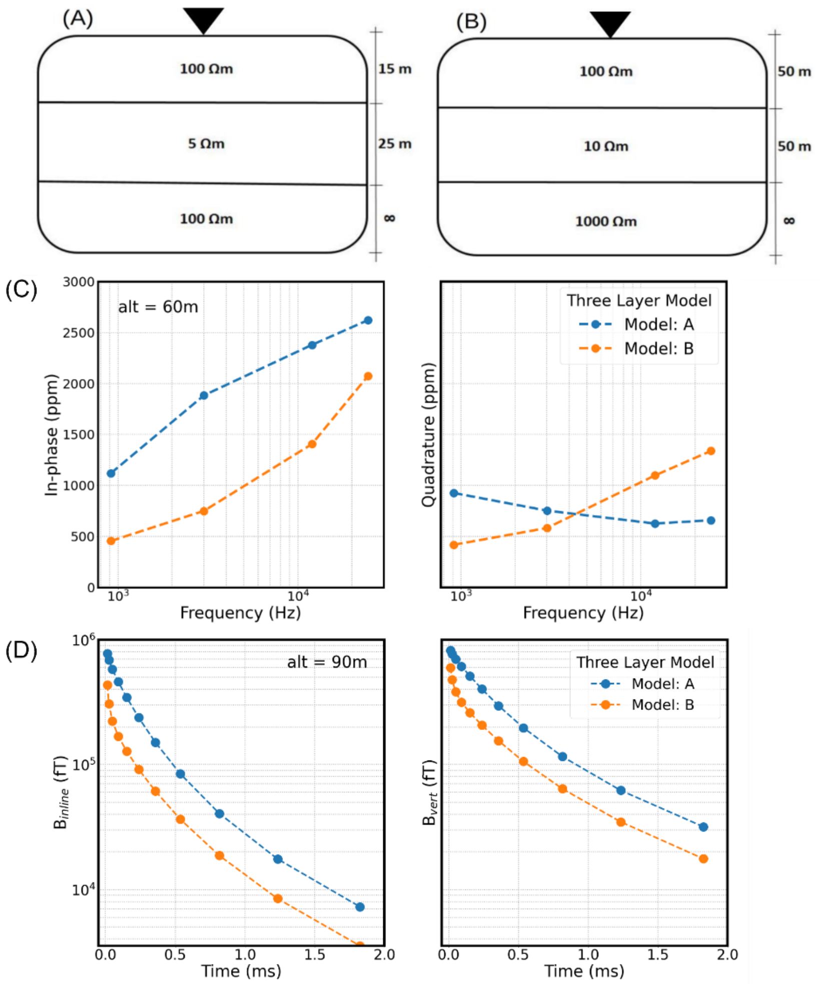

Figure 2: (A) A simple three-layer model with a lower half-space layer with a resistivity of 100Ωm. The first layer is 15m thick, with a resistivity of 100Ωm. The middle layer is 25m thick, with a resistivity of 5Ωm. (B) A simple three-layer model with a lower half-space layer with a resistivity of 1000Ωm. The first and second layers are 50m thick, with a resistivity of 100Ωm and 10Ωm respectively. (C) Computational FD forward responses of models A and B. (D) Computational TD forward responses of models A and B (Bayat, S., 2023, M.Sc. Thesis).

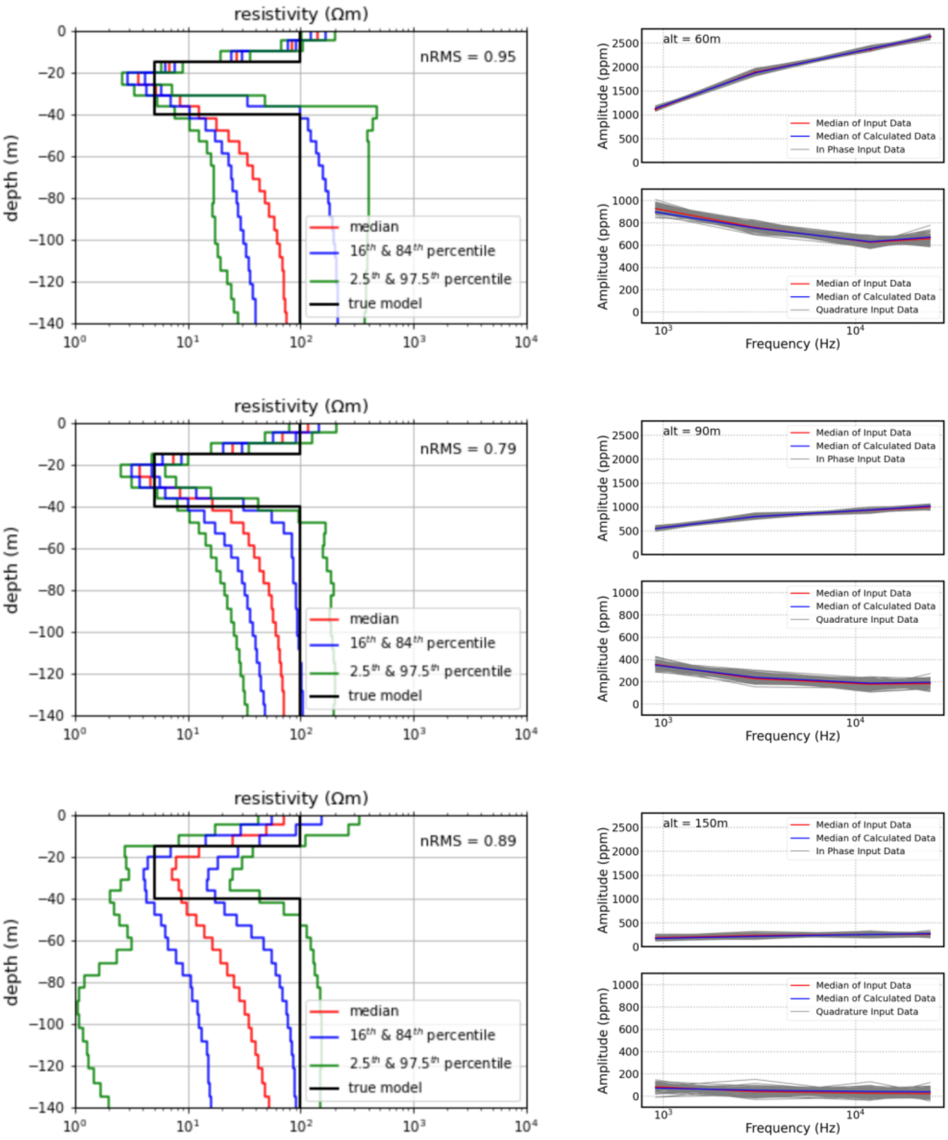

Figure 3: Tikhonov-type inversion results for a three-layer model at the altitudes of 60m, 90m, and 150m for 100 model samples of FD synthetic data. The plots on the left-hand side show the true model with the solid black line and the median resistivity values of 100 model samples with the solid red line. The bounds that contain 68 and 98 percent of the 100 model samples are shown with a blue and green solid line, respectively. The right panel illustrates the data fit. The input data responses of 100 model samples are represented with grey solid lines and the median of the data is represented with a red solid line. The median of predicted data is represented with the blue solid line. The data error assumption was 30ppm and regularisation parameters, τ_0 = 0.01, and a range of τ_1= 0.1-100 were chosen. The starting model consists of 50 layers with the thickness of the top layer starting at 5m and subsequent layers increasing logarithmically in thickness with a depth till 360m. The layer thicknesses were preserved during the inversion process. A prior resistivity of 100Ωm was chosen (Bayat, S., 2023, M.Sc. Thesis).

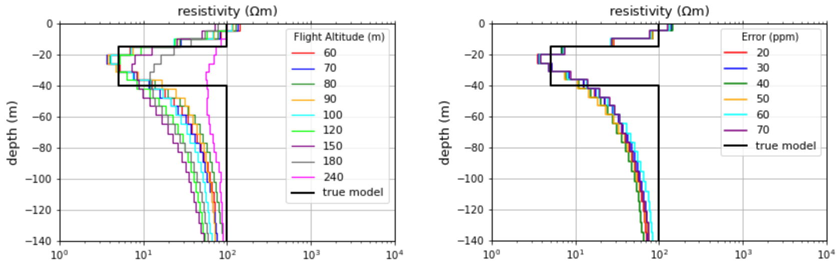

Figure 4: Summary of the output from the Tikhonov-type inversion of the synthetic FD data, which were generated with different altitude and error values (Bayat, S., 2023, M.Sc. Thesis).

A summary of all altitudes is illustrated on the left panel of Figure 4. Comparing the median value for each altitude with the true model shows a clear contrast between the recovered subsurface conductivity models for the higher altitudes (>150m). Also, the forward responses of the three-layer model with 60m flight altitude were perturbed using several error values chosen after the statistical analysis using the 240m clearance data flown in 2015 across the onshore region of the Tellus Bundoran test line (Kiyan et al., 2022). The inversion results can be seen on the right panel of Figure 4. The recovered subsurface resistivity model with 20ppm error assumption is similar to the resistivity model with 70ppm error assumption.

Forward simulations and Tikhonov-type inversion results of TD synthetic data based on the resistivity model in Figure 2B are presented in Figure 5. The in-line and vertical components of the synthetic TD data were computed at eleven Tellus survey time channels and were then randomly perturbed by the noise of 15,000fT. The flight altitudes used for the simulations are 90m, 150m, and 180m. The inversion results show that the conductive middle layer in Figure 2A has been successfully recovered. As expected, the inversion of 90m flight altitude data does a much better job of recovering the conductive middle layer. However, FD data inversion results with 60 and 90m flight altitudes more accurately recover the resistivity of the top layer.

A summary of all the altitudes is illustrated on the left panel of Figure 5. Comparing the median value for each altitude with the true model shows a clear contrast between the recovered subsurface conductivity models for higher altitudes. Similar to FD data, acquired TD data at altitudes lower than 100m do a better job when recovering the model. One can also clearly see that the FD data inversions perform better than the TD data inversions for recovering the resistivity value of the top layer. Also, the forward responses of the three-layer model with 90m flight altitude were perturbed using several error values chosen after trial-and-error. The inversion results for different data error assumptions are illustrated on the right panel of Figure 5.

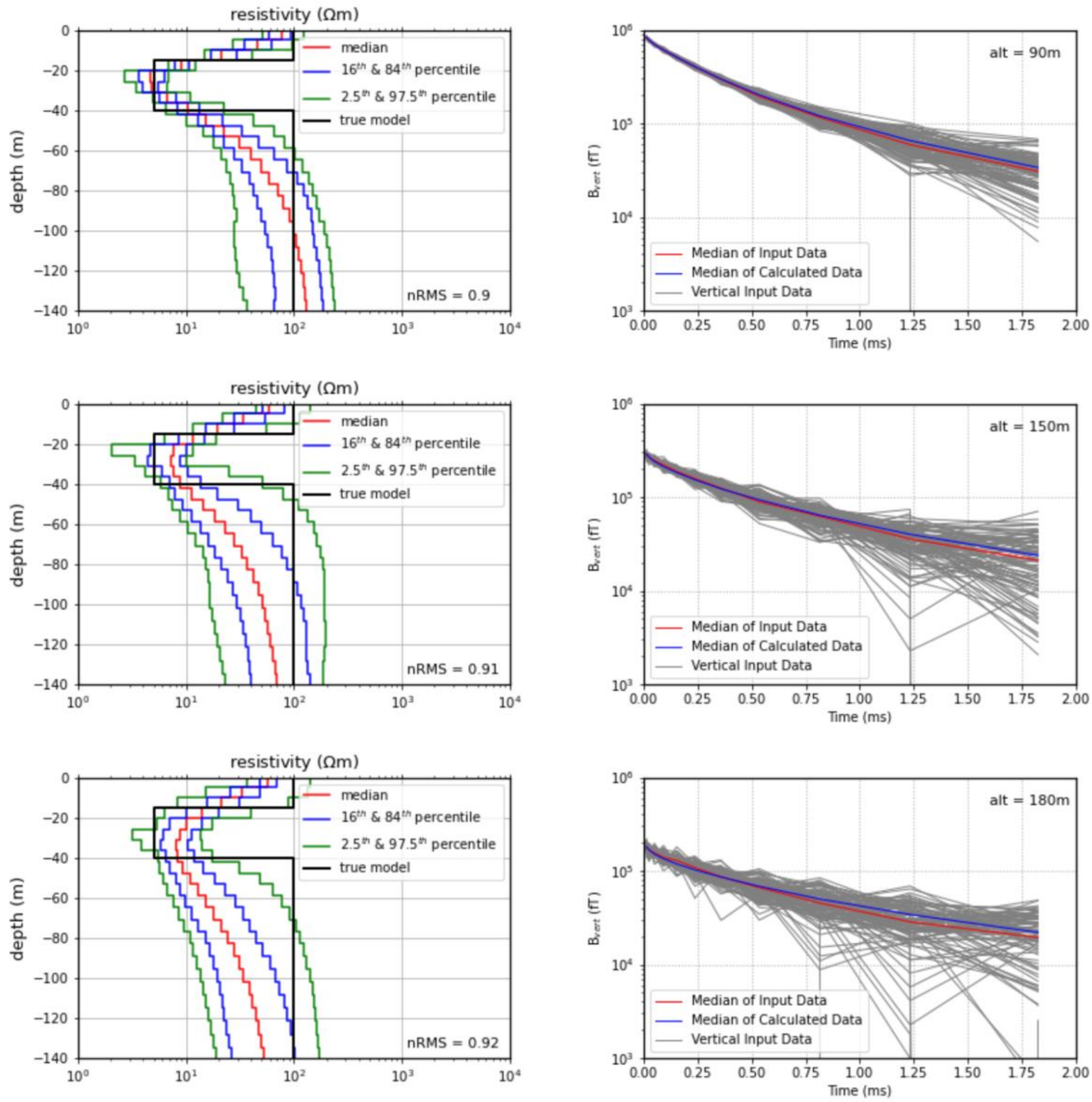

Figure 5: Tikhonov-type inversion results for a three-layer model at the altitudes of 90m, 150m, and 180m for 100 model samples of TD synthetic data. The plots on the left-hand side show the true model with the solid black line and the median resistivity values of 100 model samples with the solid red line. The bounds that contain 68 and 98 percent of the 100 model samples are shown with a blue and green solid line, respectively. The right panel illustrates the data fit and median of the data. 100 model samples are represented with grey solid lines and the median of the data is represented with a red solid line. The median of predicted data is represented with the blue solid line. The data error assumption was 15,000fT and regularisation parameters, τ_0 = 0.01, and a range of τ_1 = 0.1-100 were chosen. The model consists of 50 layers with the thickness of the top layer starting at 5m and subsequent layers increasing logarithmically in thickness with a depth till 360m. The layer thicknesses were preserved during the inversion process. A prior resistivity of 100Ωm was chosen (Bayat, S., 2023, M.Sc. Thesis).

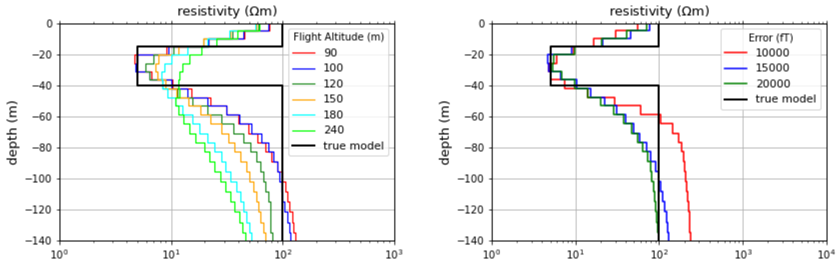

Figure 6: Summary of the output from the Tikhonov-type inversion of the TD data, which were generated with different altitude and error values (Bayat, S., 2023 M.Sc. Thesis).

Considering that TD data generally provide much deeper resolution compared to FD data, and is more sensitive to greater depths, TD data have also been simulated and inverted based on the simple three-layer resistivity model in Figure 2B. In-line and vertical components of the synthetic TD data were computed at eleven Tellus survey time channels and were then randomly perturbed by the noise of 3,000fT. The flight altitudes used for the simulations are 90m, 150m, and 180m. The inversion results in Figure 7 show that the resistivity and the thickness of the first two layers have been recovered successfully. However, the resistivity of the bottom layer has not been accurately resolved. Inclusion of the highly conductive middle layer decreases the resolution of the bottom layer. A summary of the results for all altitudes is illustrated on the left panel of Figure 8. The forward responses of the three-layer model generated with the flight altitude of 90m were perturbed using several error values chosen after trial-and-error. The inversion results for different data error assumptions are illustrated on the right panel of Figure 8.

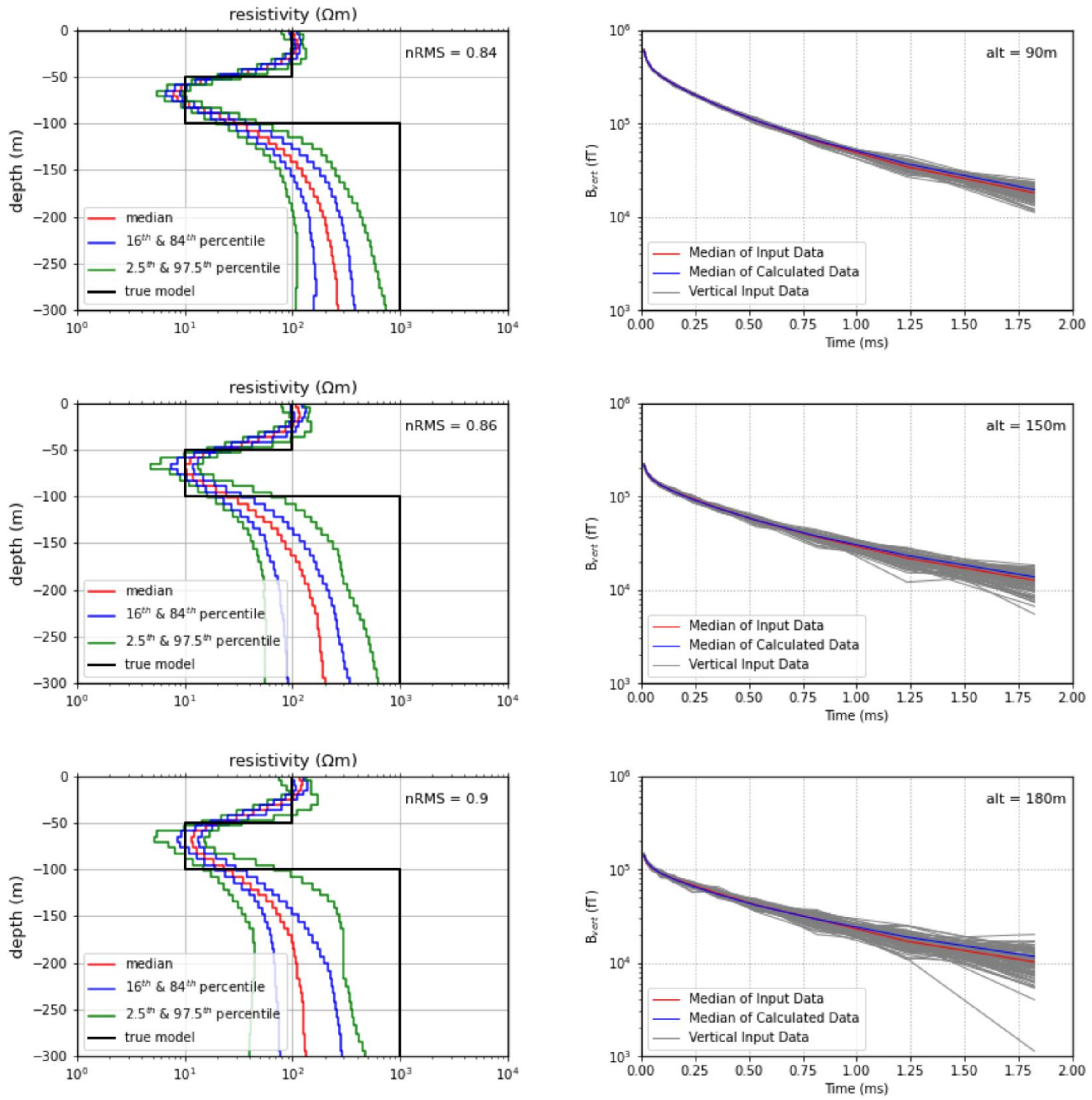

Figure 7: Tikhonov-type inversion results for a three-layer model at the altitudes of 90m, 150m, and 180m for 100 model samples of TD synthetic data. The plots on the left-hand side show the true model with the solid black line and the median resistivity values of 100 model samples with the solid red line. The bounds that contain 68 and 98 percent of the 100 model samples are shown with a blue and green solid line, respectively. The right panel illustrates the data fit and median of the data. 100 model samples are represented with grey solid lines and the median of the data is represented with a red solid line. The median of predicted data is represented with the blue solid line. The data error assumption was 3,000fT and regularisation parameters, τ_0 = 0.01, and a range of τ_1 = 0.1-100 were chosen. The model consists of 50 layers with the thickness of the top layer starting at 5m and subsequent layers increasing logarithmically in thickness with a depth till 360m. The layer thicknesses were preserved during the inversion process. A prior resistivity of 100m was chosen (Bayat, S., 2023, M.Sc. Thesis).

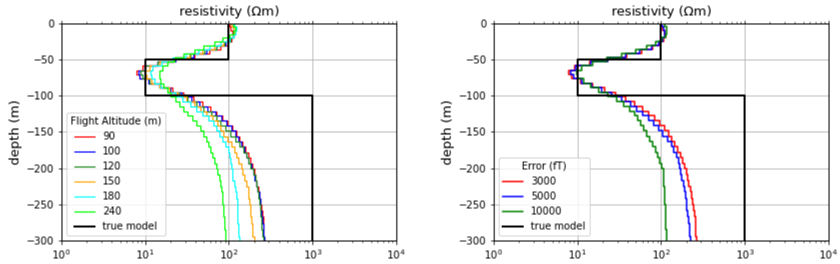

Figure 8: Summary of the output from the Tikhonov-type inversion of the TD data, which were generated with different altitude and error values (Bayat, S., 2023, M.Sc., Thesis).

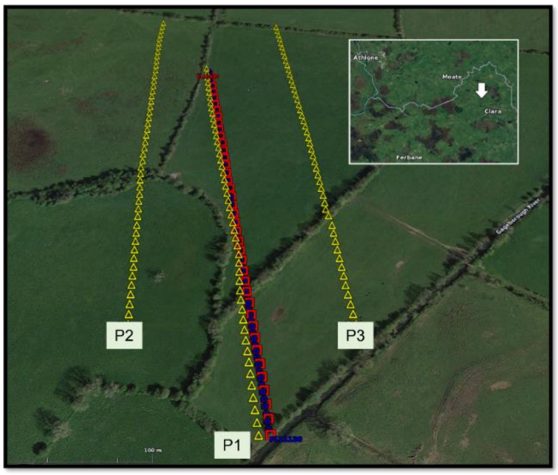

Figure 9: Location map of the study area with the frequency- and time-domain AEM data measurement points and the ERT profiles. The center profile (P1) is almost identical to the overlap flight line, where both FD and TD data are available. In order to get a quasi-3-D picture of the subsurface, two parallel ERT profiles were measured at a distance of approximately 100m.

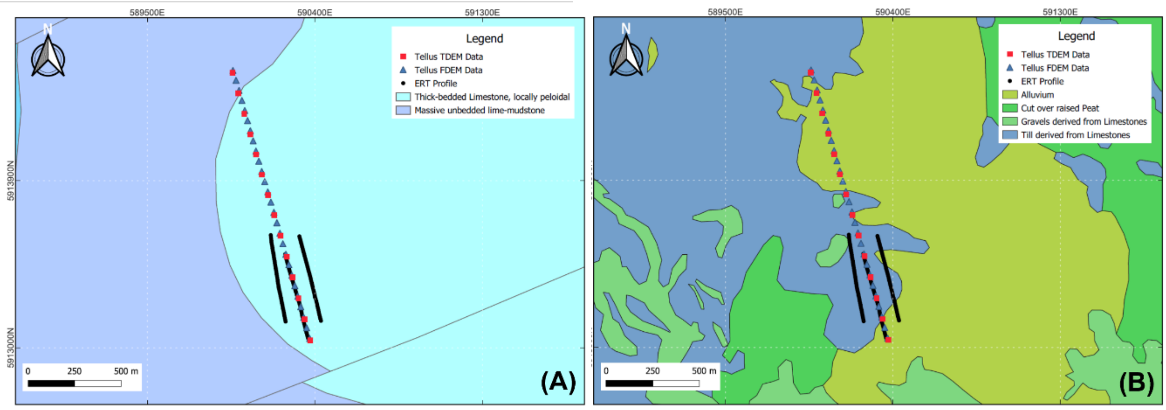

Figure 10: Quaternary and Bedrock Geology (GSI, 1:100,000) maps of the study area with the locations of FD- and TD AEM data measurement points and the ERT profiles. The maps were created with QGIS. (Bayat, S., 2023, M.Sc. Thesis).

Tellus FD and TD airborne datasets were inverted from flight lines No: L1126 and No: L13490, respectively (Figure 11). 1-D models of resistivity variations with depth were derived independently and were subsequently gridded together to produce pseudo 2-D resistivity sections. Inversions were carried out using both in-phase and quadrature components of FD data at four frequencies. The data error assumption was 50 ppm. Note that the inverted models derived from the FD data were reconstructed using the first two singular values and vectors (Kiyan et al., 2022). Note that TD data inversions were carried out with the vertical (Z) component data only, as the in-line (X) component data are smaller than the vertical data and the negative values occur mainly in the X component.

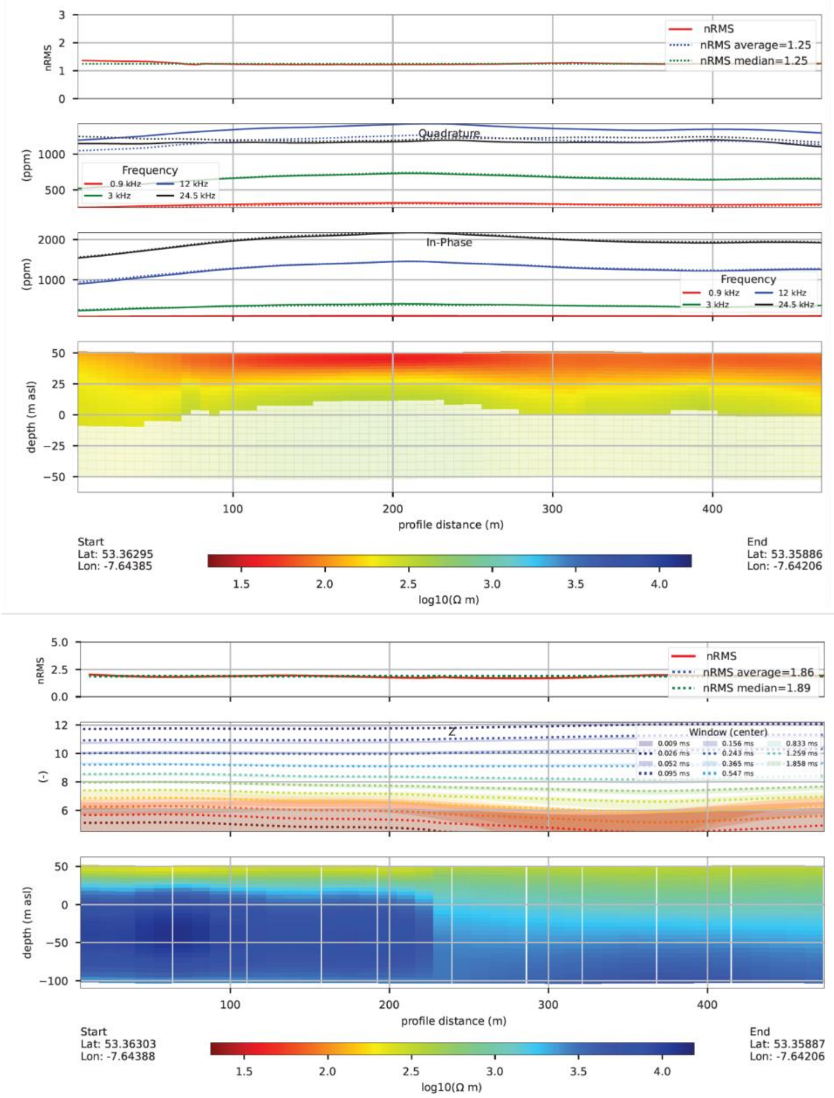

Figure 11: Electrical resistivity models from the inversion of Tellus FD (top) and TD (bottom) data consistent with the main ERT profile from the Clara survey area. The limit for sensitivity-based shading is 10^{-3}. The description of sensitivity calculations implemented in the AEMpyX can be found in the AEMpyX manual (Kiyan, Rath et al., 2023). Inversion regularisation parameters $\tau_0 = 0.01$ and $\tau_1 = 0.1$-100 were chosen. For the FD data inversions, the starting model consists of 32 layers with the thickness of the top layer starting at 2m and subsequent layers increasing logarithmically in thickness with depth till 160m. The layer thicknesses have been preserved during the inversion process. A prior resistivity of 100Ωm was chosen, and each site was modelled independently. For the TD data inversions, the starting model consists of 30 layers with the thickness of the top layer starting at 4m and subsequent layers increasing logarithmically in thickness with depth till 160m. The layer thicknesses have been preserved during the inversion process. A prior resistivity of 300Ωm was chosen, and each site was modelled independently. (Bayat, S., 2023, M.Sc. Thesis).

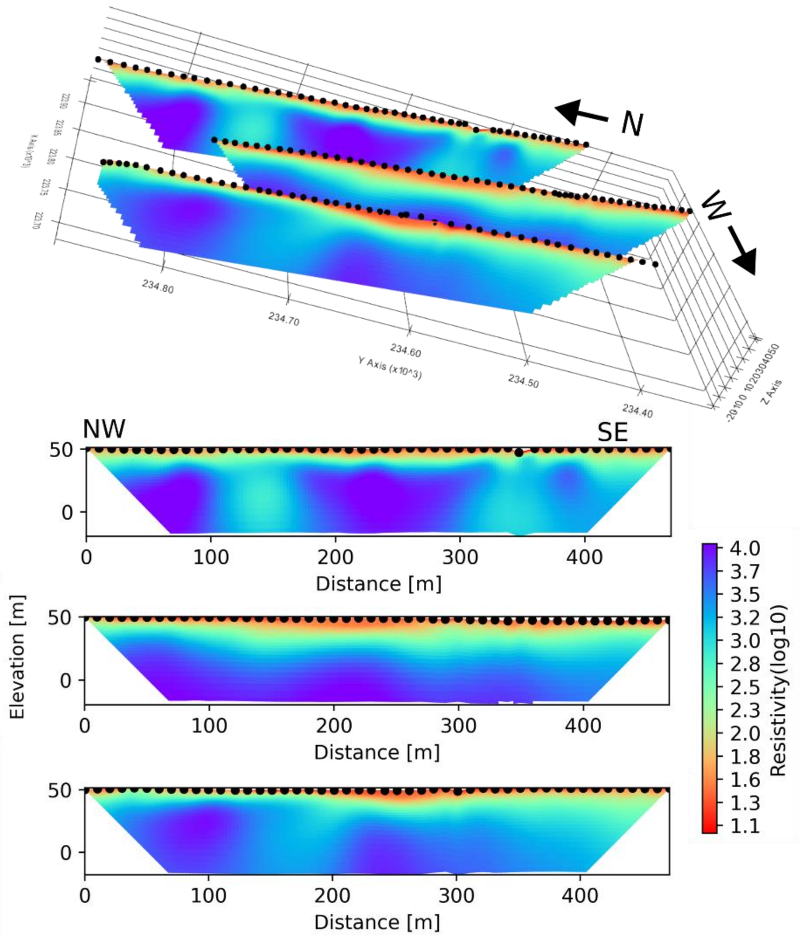

Figure 12: Electrical resistivity models from the inversion of ERT data using ResIPy software (Blanchy et al., 2020). ERT data were acquired with a 10m spacing between electrodes using Wenner-Schlumberger configuration (modified from Bayat, S., 2023, M.Sc. Thesis).

The bedrock geology along the 470m portion of the AEM profiles is mapped as the Allenwood Formation (massive, unbedded lime-mudstone). The resistivity model derived from the ERT data along the main profile shows a highly resistive bedrock with resistivities greater than 5000Ωm. The ERT model agrees with the time-domain AEM derived resistivity model, which also shows a highly resistive bedrock with a resistivity greater than 3000Ωm. The ERT-derived resistivity models show a conductive layer with a thickness of about 10m along the three profiles. The thickness of this conductive layer increases at the centre of the main profile. According to the GSI Quaternary Sediments map till derived from limestones is the predominant subsoil types along the profiles. The much less resistive material (approximately 300–500Ωm) along the whole profile between the depths of 40–30m.a.s.l. could correspond to this subsoil type. The FD resistivity model shows a more conductive (approximately 50–150Ωm) till units to a depth of about 25m.a.s.l. overlying a transition zone in which resistivities increase with depth. However, the resistivity model has a lower resolution than the ERT-derived and time-domain AEM-derived resistivity models.

(ii) Implementation

AEMpyX (Figure 13) has been developed and implemented within the framework of RAFTA and can be seen as a follow-up to the original *aempy* toolbox development.

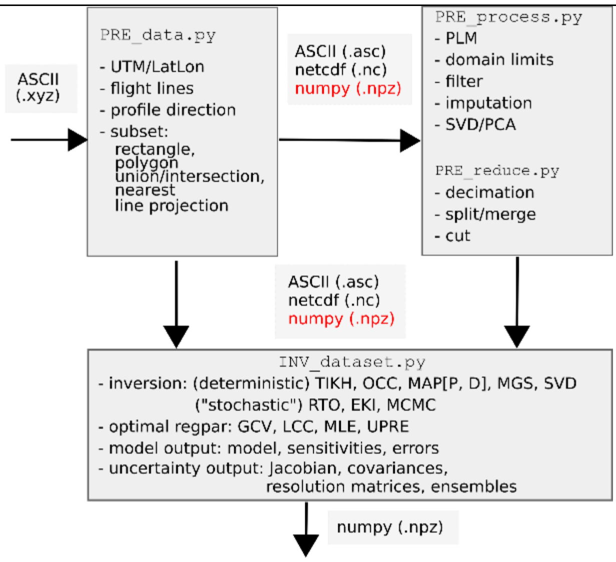

Figure 13: A simplified diagram showing AEMpyX workflow. Detailed information can be found in the AEMpyX manual (Kiyan, Rath et al., 2023).

The main objective of the proposed project has been achieved through individual Work Packages (WPs) as follows:

WP-1: Data preparation for inversion and resolution analysis. This WP aims at the hitherto unfinished inclusion of the TD data from the TNM block. These data have been compared to the FD data within the overlap zones A1, A2, and TB (Kiyan, Rath et al., 2023).

WP-2: Quantitative analysis of AEM data errors. This WP targets the development of reasonable error models and estimates for both FD and TD systems. This implies the use of synthetic data from forward simulations for appropriate 1-D and 2-D subsurface models. Different error models have been considered for the forward simulations. The synthetic data have then been inverted using existing deterministic approaches (Figure 14) implemented within AEMpyX.

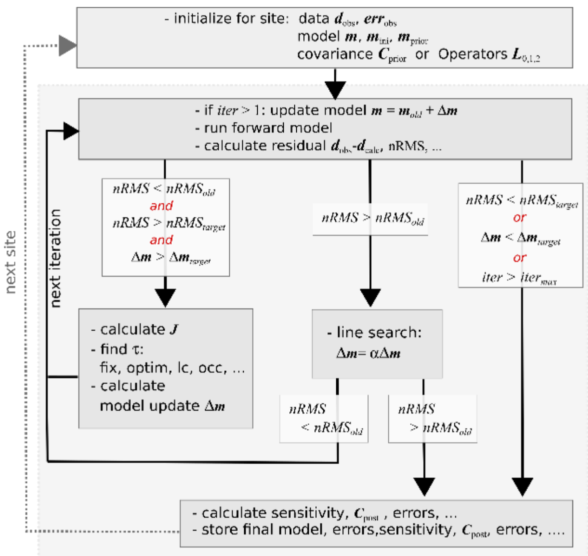

Figure 14: Flowchart for the Tikhonov-type inversion implemented in AEMpyX. Descriptions are given in the AEMpyX manual (Kiyan, Rath et al., 2023).

WP-3: Uncertainty and resolution analyses for FD and TD AEM data. This WP targets development and implementation of workflows for uncertainty and resolution analysis for AEM interpretation in the FD- and TD-domain (Kiyan, Rath et al., 2023).

(iii) Outputs to date (this should include the location of datasets generated, as per GSI and NORF requirements)

1) The AEMpyX (extended version of aempy) toolbox and the Manual (Inversion and Uncertainty Quantification for Airborne Electromagnetic Data: The AEMpyX Toolbox). The AEMpyX_public github repository is currently being tested.
   The toolbox can be downloaded from the following link on 1 September 2023: https://github.com/RAFTA-AIRBORNE/AEMpyX_public.git
2) ERT data and models from the Clara Survey Area, Co. Offaly.
3) Synthetic AEM data and model plots can be found in Bayat, S., 2023, M.Sc. Thesis.
4) Tellus FD and TD AEM data used in this project are hosted on the DIAS repository.
5) Tellus FD and TD models generated in this project are hosted on the DIAS repository.

(iv) Impact

- Relevance/application to GSI programmes, where applicable
  - GSI Tellus team is currently producing and making available to the public EM resistivity inversion models computed using the *aempy* code. *aempy* can now be replaced with the AEMpyX (“aempy-extended”) toolbox.
  - The outcomes of the project should undoubtedly improve the characterisation of the near-surface geology and identification of hydrogeological features, namely the physical properties and thickness of surficial sediments in Ireland that are crucial for defining, protecting, and managing our landscape and aquifers. We believe that the outcomes of this project will be useful for research themes identified by GSI such as Groundwater resources and protection, Quaternary geology, Mineral exploration, and Bedrock geology.
  - The depth of investigation (<100m) provided by the AEM data should allow investigation of subsurface features which will be of use to bedrock mapping, Quaternary mapping, hydrological studies, environmental studies, civil engineering investigations, geothermal assessments for ground-source heat pump installations, and mineral, dimension-stone and aggregate exploration.

- Other impacts (these should be medium-long term impacts, not the project outputs)
  - The AEMpyX toolbox is open-source (facilitated by its coding in Python) making it freely available under GNU General Public License, Version 3 (2007) – thereby supporting the ethos and intent in the free public release of the Tellus airborne datasets by GSI – and freely adaptable for application to other AEM systems or for other research objectives. The scripts developed for model uncertainty and resolution analyses will be implemented within AEMpyX and can be also used for training and education purposes.
  - The resolution analyses implemented in this project should help interpreters of the electrical conductivity models better understand what types, scales and depths of geological structures are reliably imaged, leading to better interpretations with

higher confidence levels. It will also help those inverting the data themselves to produce more reliable inversion models, as choice of appropriate inversion parameters can be guided by a knowledge of the resolution capabilities of the data.

Acknowledgements:

We would like to thank Australia's CSIRO and the Amira International consortium for making their P223 modelling suite open access. We are especially thankful to David O'Leary and Eve Daly from NUI Galway and Clodagh Moriarty from DIAS, who helped with the ERT fieldwork.

References:

Bayat, S. Resolution analyses for the tellus airborne electromagnetic data compared with co-located electrical resistivity tomography data. M.Sc. Thesis, School of Natural Sciences, National University of Ireland – Galway, Ireland, 2023.

Blanchy, G., S. Saneiyan, J. Boyd, P. McLachlan, and A. Binley. ResIPy, an intuitive open-source software for complex geoelectrical inversion/modelling, 2020. Computers & Geosciences, 104423, doi: 10.1016/j.cageo.2020.104423. 23, 35

Kiyan, D., V. Rath, M.R. Muller, M.D. Ture, and J. Hodgson. 1-D inversion of frequency-domain airborne electromagnetic data using the open-source aempy toolbox, 2022. Journal of Applied Geophysics, 198, https://doi.org/10.1016/j.jappgeo.2022.104562.

Kiyan, D., V. Rath, S. Bayat, and M.R. Muller. Inversion and Uncertainty Quantification for Airborne Electromagnetic Data: The AEMpyX Toolbox, 2023.

Publications:

(Poster) Bayat, S., D. Kiyan, V. Rath, M.R. Muller, and E. Daly, 2022. The Rafta Project: Resolution Analyses for Frequency- and Time-domain Airborne Electromagnetic Data of the Irish Tellus Programme, 65th Irish Geological Research Meeting, virtual event, 25 February.

(Poster) Bayat, S., D. Kiyan, V. Rath, M.R. Muller, and E. Daly, and Jim Hodgson, 2023. Understanding the Capabilities of the Tellus Frequency- and Time-Domain Airborne Electromagnetic Data, 66th Irish Geological Research Meeting, Ulster Museum, Belfast, UK, 3-5 March.

(M.Sc. Thesis) Bayat, S., 2023. Resolution Analyses for the Tellus Airborne Electromagnetic Data Compared with Co-located Electrical Resistivity Tomography Data. *M.Sc. Thesis*, School of Natural Sciences, National University of Ireland – Galway, Ireland. Supervisors: Dr Duygu Kiyan (DIAS) and Dr Eve Daly (NUIG).